Tellus SERIES A DYNAMIC METEOROLOGY AND OCEANOGRAPHY
PUBLISHED BY THE INTERNATIONAL METEOROLOGICAL INSTITUTE IN STOCKHOLM

Simulations of the Bergen orographic wind shelter

By MARIUS O. JONASSEN[1]*, HARALDUR ÓLAFSSON[1,2], ASLAUG S. VALVED[1], JOACHIM REUDER[1] and JAN A. OLSETH[1], [1]*Bergen School of Meteorology, Geophysical Institute, University of Bergen, Allégaten 70, Bergen, Norway*; [2]*Department of Physics, University of Iceland, Icelandic Meteorological Office, Bústaðavegi 9, IS-150 Reykjavík, Iceland*

(Manuscript received 27 July 2012; in final form 31 May 2013)

ABSTRACT

Even though the coast of western Norway is very windy, the centre of Bergen is rather calm. To gain further understanding of this wind shelter, we study the flow in the complex topography of Bergen during two south-westerly windstorms using surface observations and high-resolution numerical simulations. The results reveal large spatial variability in the local wind field. In some areas, there are periods of sustained winds of more than 25 m s^{-1}, while at nearby locations the winds are typically less than 5 m s^{-1}. The centre of Bergen is among the calmest areas. To investigate the effect of the individual mountains upstream (Løvstakken) and downstream (Fløyen) on the wind field in the city centre of Bergen, they have been removed stepwise from the model topography. Areas with relatively large wind speed reductions are found immediately downstream of Løvstakken and immediately upstream of Fløyen. At Florida, situated close to the city centre, both a wake effect of Løvstakken and a blocking effect of Fløyen are evident, but the latter is more prominent. The total impact of both mountains on the winds in the city is close to the sum of each of them. A spillover effect of Løvstakken acts to substantially increase the local precipitation in the centre of Bergen. The spillover effect is presumably less pronounced for cases with weaker winds.

Keywords: complex terrain, wake, blocking, precipitation, southwestern Norway

1. Introduction

The centre of Bergen, as represented by the weather station 'Florida', appears to be remarkably sheltered during strong south-westerly flow (Harstveit, 2006; Jonassen et al., 2012). It is, however, unclear if this sheltering effect (hereby referred to as the 'Bergen shelter') is caused by a wake of the upstream mountain massif of Løvstakken (e.g. Smith et al., 1997), a blocking by the downstream mountain massif of Fløyen or a combination of both. It is also unclear whether the wind observations at Florida are representative for the city centre of Bergen as a whole. These are the main questions to be answered in this study. The results may serve as guidance for studies of local dispersion of pollutants and weather forecasting in the area.

There are numerous studies on how larger scale flow is affected by the south Norwegian mountain range. Such investigations were initiated already during the early days of the Bergen School of Meteorology (Bjerknes and Solberg, 1921, 1922). Their studies were continued by Spinnangr (1943) and Andersen (1975). More recently, Barstad and Grønås (2005, 2006) identified and explained several meso-scale flow structures frequently forming over and around the topography of southern Norway for flow within the sector south to west. However, studies on local scale flow in the Bergen area are few and focus mainly on thermally driven winds (Utaaker, 1995) and temperature inversions (Berge and Hassel, 1984).

Many of the flow patterns forming in connection to topography can be diagnosed using the non-dimensional mountain height $\hat{h} = Nh/U$ (e.g. Pierrehumbert and Wyman, 1985), where N is the Brunt–Väisälä frequency, describing the buoyancy on a vertically displaced air parcel, h is the mountain height and U is the flow speed of the airmass impinging on the mountain (e.g. Peng et al., 1995; Trüb and Davies, 1995; Lin and Wang, 1996; Ólafsson and Bougeault, 1996). High values of $\hat{h}$ facilitate for blocked flow leading to more of the flow going around than over the mountain. In such flow, there may be prominent sheltering from ambient winds inside either an upstream blocking or a downstream wake. For low values of $\hat{h}$, the flow typically passes over the mountain and weak

*Corresponding author.
email: marius.jonassen@gfi.uib.no

Citation: Tellus A 2013, **65**, 19206, http://dx.doi.org/10.3402/tellusa.v65i0.19206

gravity waves may form. In the complex topography of south-western Norway, these flow patterns frequently form at the larger scale as documented in the aforementioned literature. The same flow patterns should be expected to form at the lesser documented smaller scale, which we focus on in this study.

Topographically modified flow also affects precipitation (e.g. Jiang, 2003; Smith, 2006). Orographic precipitation (i.e. precipitation that is formed as moist air is forced to ascend over mountains) is an integral part of the climate of western Norway, both in terms of mean values (e.g. Reuder et al., 2007) as well as extremes (Steensen et al., 2011). The phenomenon is of essential importance to a range of environmental factors of both direct and indirect influence on people, such as the local hydrology, long-term trends in terrain evolution, development of glaciers, etc. Mountains enhance precipitation on their upwind side, but this enhancement may extend downstream of the mountains' crest as the precipitation elements are transported downwind while forming and falling to the ground (the 'spillover effect') (e.g. Sinclair et al., 1997). The mean annual precipitation in the city of Bergen is 2250 mm, which is almost twice the value of precipitation at locations along the Norwegian southwest coast that are far away from mountains, such as Stavanger (1250 mm). It is well recognized that the larger scale topography of southern Norway has a central role in creating the high precipitation amounts along the southwest coast of Norway where Bergen is situated (e.g. Teigen, 2005). It is, however, not clear how large the contribution from the local topography is, for example, through the above-described spillover effect.

The primary purpose of this article is to investigate the above-introduced Bergen shelter effect. As a by-product of this investigation, some results on precipitation will be presented. We study the local flow field in Bergen during two south-westerly windstorms that hit the southwest coast of Norway on 10 January 2009 (Case 1) and 25 December 2011 (Case 2). Data from a dense network of automatic weather stations (AWS) along with high-resolution numerical simulations with the Weather Research and Forecasting model (WRF) (Skamarock et al., 2008) are used. The latter storm, named Dagmar by the Norwegian Meteorological Institute (met.no), caused floodings, property damage, and even casualties along the coast in the areas most severely affected. We find the former windstorm to be a more typical storm for the winter season in the region.

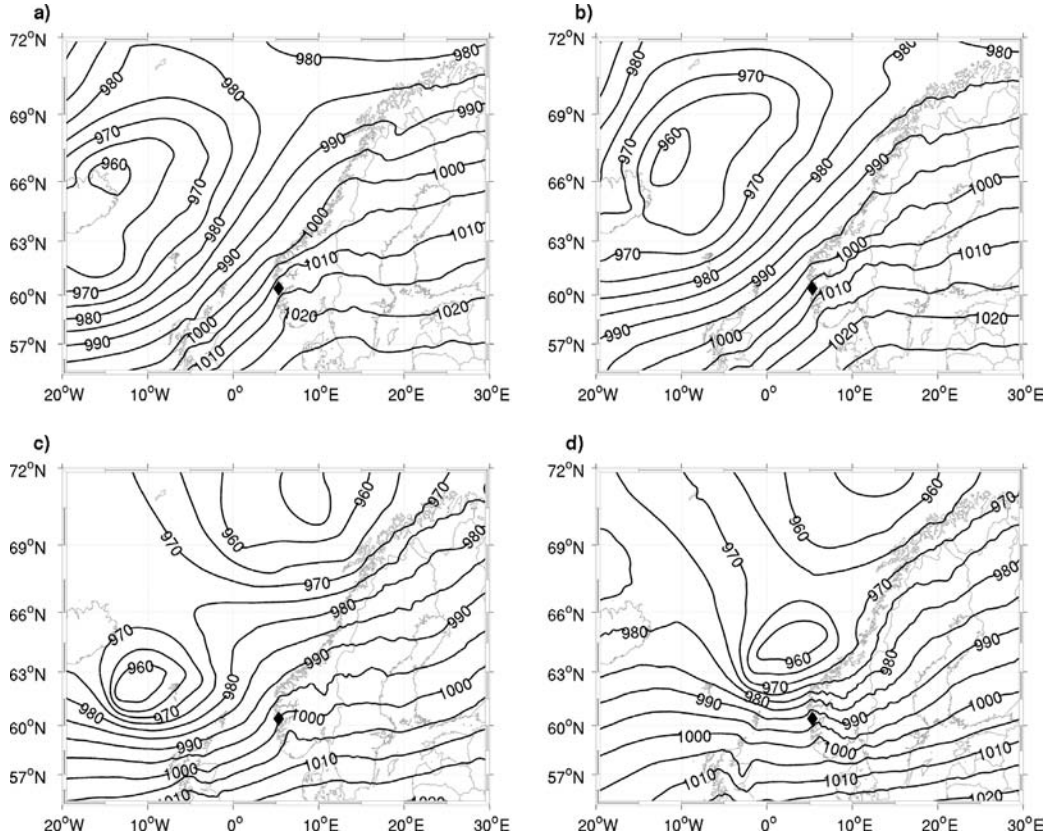

Fig. 1. Mean sea-level pressure at 1200 and 1800 UTC on 10 January 2009 (a, b) and 25 December 2011 (c, d) based on the analysis from the European Centre for Medium-Range Weather Forecasts (ECMWF). The location of Bergen is indicated with a black diamond.

Table 1. Automatic weather stations

Station	Time res. (min)	Source	m.a.s.l.	m.a.g.l.
Florida	10	GFI	48	30
Ulriken	10	AADI/GFI	605	15
Flesland	60	met.no	48	10
Sotra bridge	10	NPRA	50	50
Sotra	60	Avinor	341	10
Ulriksbakken	10	GFI	408	2.5
Haukeland	10	GFI	64	10
Løvstakken	10	GFI	472	2.5
Strandafjellet	10	GFI	303	2.5
Nordnes	10	GFI	48	30

The height for Ulriken is set to 15 m.a.g.l., representing an average elevation above its immediate surroundings. NPRA = Norwegian Public Roads Administration; AADI = Aanderaa Data Instruments AS.

2. Atmospheric data

2.1. Case studies: two south-westerly windstorms

On 10 January 2009, a low-pressure system to the south of Iceland and a high-pressure system over central Europe induced strong south-westerly flow along the coast of south-western Norway (Fig. 1). This low-pressure system moved slowly towards the northeast and the associated flow over the Bergen area remained fairly stationary throughout the day. However, the system of 25 December 2011 moved rather quickly eastwards. The general flow direction over south-western Norway thus shifted from south-westerly in the beginning of the day to westerly towards the evening.

2.2. Observations

There is a fairly dense network of AWSs in the Bergen area. The main AWS in Bergen is situated in the city centre and called 'Florida'. At Florida, the observations are made on the top of the building of the Geophysical Institute (GFI), University of Bergen, around 30 m above the surrounding ground. There is also a station on the top of the highest nearby mountain, Mount Ulriken. In addition, there is an AWS at the airport of Flesland, some 10 km to the south of Florida, and at Mount Sotra, situated to the west of the latter. Another station is situated at the Sotra bridge. All these stations were in service during the windstorm on 10 January 2009. From the windstorm on 25 December 2011, data from a network of five additional stations in Bergen are available from a research project at GFI. Detailed statistics on the observations from Florida and

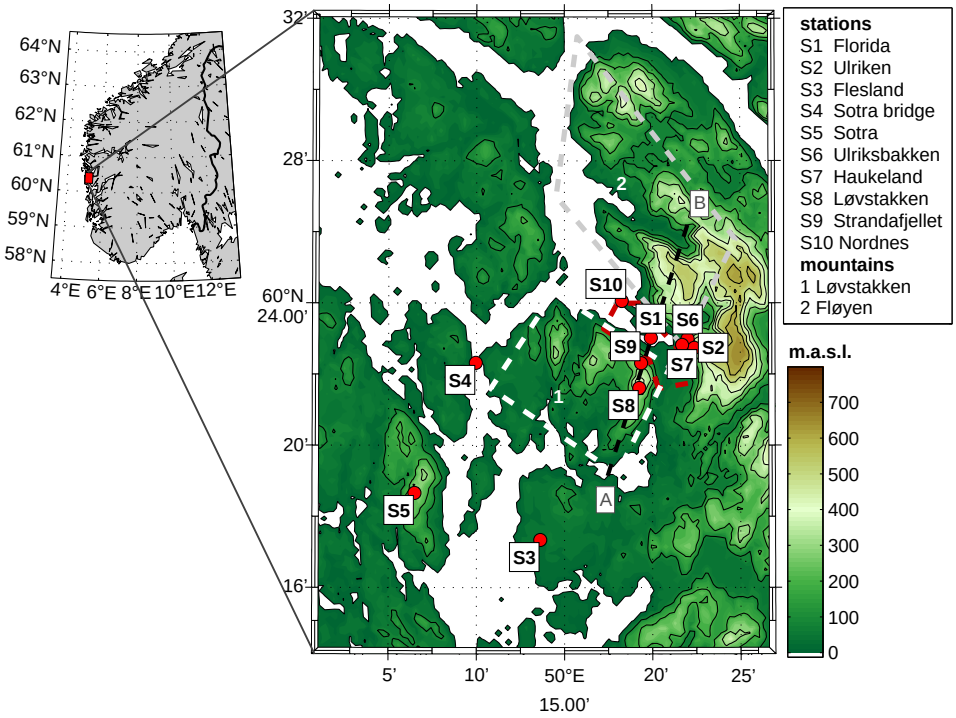

Fig. 2. The topography of the area of main interest, the locations and names of the AWSs (S1–S10), and indications of the geographical extent of the two dominating mountain massifs in the area: Løvstakken (1) and Fløyen (2). The dashed, red line indicates the approximate extent of the centre of Bergen. The dashed, black line between the points 'A' and 'B' indicates the position of the cross section in Fig. 14.

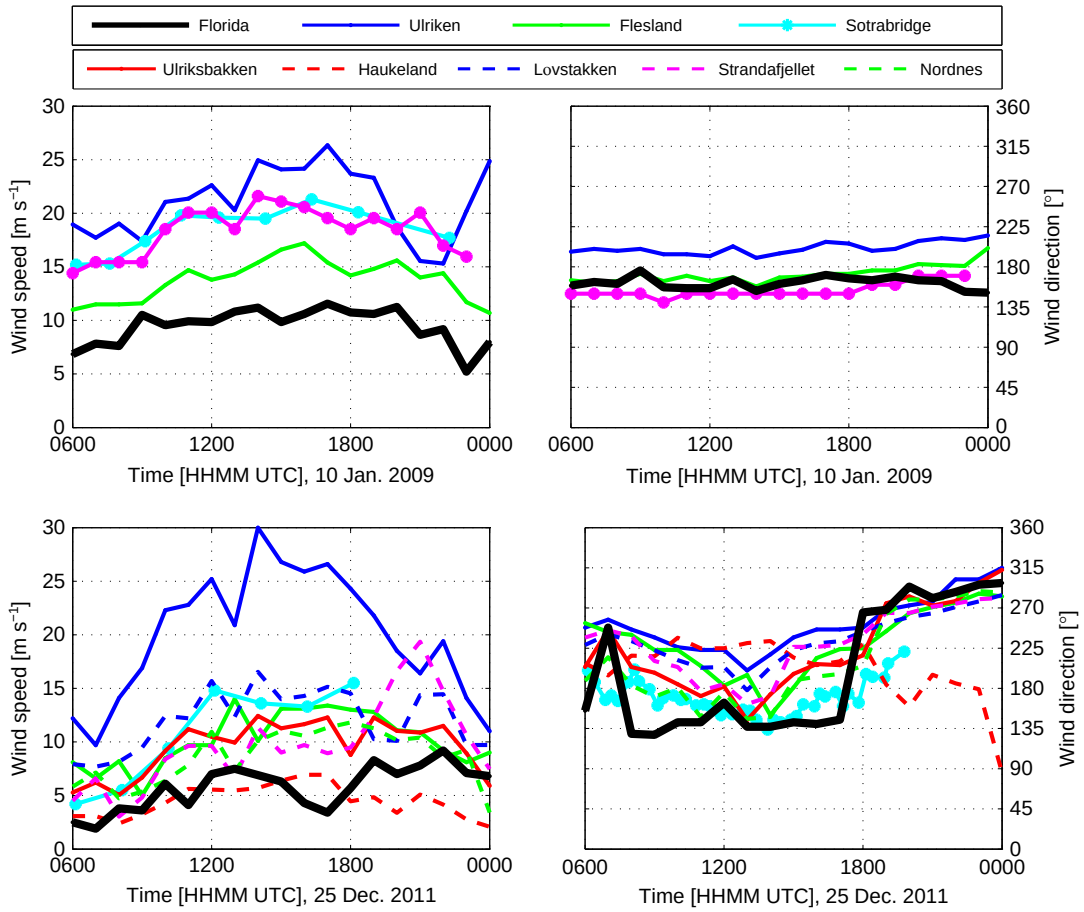

Fig. 3. Observed wind speed and wind direction during the investigated windstorms on 10 January 2009 and on 25 December 2011 in the Bergen area.

Ulriken can be found in Jonassen et al. (2012) and Valved (2012). An overview of the AWSs is given in Table 1 and their geographical locations are indicated in Fig. 2.

The observed wind speed presented in the following is from the unprocessed raw data. In the later comparison with the simulated wind speed, however, we have converted the observed wind speed (u_z) to the height of the lowermost half sigma level in the WRF model setup ($z = 19.5$ m.a.g.l.) using the following formula, which describes a logarithmic wind profile:

$$u_z = \frac{u_*}{\kappa}\left[\ln\left(\frac{z-d}{z_0}\right) + \psi(z, z_0, L)\right]$$

Here, u_* is the friction velocity (m s^{-1}), defined as $u_* = \sqrt{\left(\frac{\tau}{\rho}\right)}$ where τ is the Reynolds stress and ρ is air's density, while z_0 is the roughness length in metres. The value of z_0 used for each AWS is indicated in Fig. 4. d is the zero displacement length (m), that is, the height adjacent to the obstacle (here a building) at which the wind speed is zero. Furthermore, d is set to 2/3 of z, where z is 30 m for Florida and Nordnes. In the calculations, we have assumed neutral atmospheric stability implying that the stability term $\psi(z, z_0, L)$ is set to zero. In $\psi(z, z_0, L)$, L is the Monin–Obukhov stability parameter.

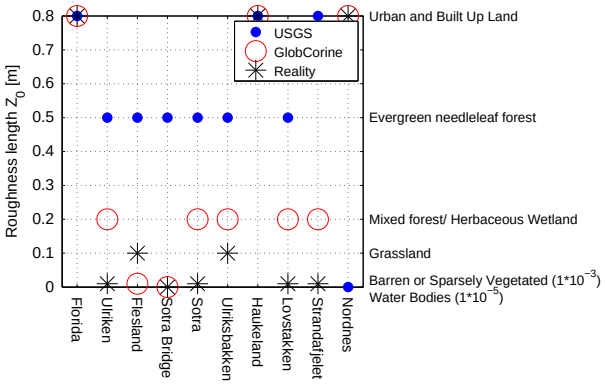

Fig. 4. Roughness length for momentum at the different AWSs for the simulations using the USGS and GlobCorine land-use data sets. The real roughness length is indicated as well.

Assuming neutral stability is presumably a close approximation to reality because the investigated weather situations contain relatively high wind speeds, thus providing significant turbulent mixing of momentum.

During the two studied windstorms, the AWS observations reveal a large spatial variability in the wind field in the area (Fig. 3). While the wind speed at the top of Mount Ulriken reaches more than 25 m s^{-1} in both cases, the wind speed at Florida, situated in the middle of the Bergen valley, barely exceeds 12 m s^{-1} in any of the cases.

The results from Case 2 allow for a more detailed investigation of the wind in the centre of Bergen because they include more AWS observations from the area. The wind speed observed in the northern part of the city centre (Nordnes) is stronger than at Florida. It is in fact more similar to the wind speed observed at Flesland, which is situated some 10 km to the south of Florida and is more exposed to the strong winds.

While the wind speed at most AWSs decreases as the flow turns westerly in Case 2 (after 1800 UTC), it remains the same or is even slightly higher at Florida (the same is seen at the mountain stations of Strandafjellet and Løvstakken). When compared to the wind direction at Ulriken, which is on average found to be in reasonable agreement with the larger scale flow direction (Jonassen et al., 2012), the wind direction observed at the other AWSs show large deviations towards a more south and south-easterly direction for the south-westerly flow of Case 1. In the south-westerly flow of Case 2 (before 1800 UTC), the deviations are even larger and it is particularly large at Florida. This deviation is undoubtedly caused by the strong alignment of the flow to the Bergen valley at this location. However, in the westerly flow of Case 2 (after 1800 UTC) there is a clear agreement in the wind direction for all stations. An exception is the AWS at Haukeland, where the wind speed is very low at this time.

2.3. *Numerical simulations*

To further investigate the local wind in the Bergen area during the two studied windstorms and how it is modified by the surrounding topography, we have numerically reproduced the flow during both case studies with high horizontal resolution using the WRF model. The modelling system is fully compressible and is in this study run in non-hydrostatic mode using three one-way nested domains with horizontal resolutions of respectively 4.5, 1.5 km and 500 m. The outermost and coarsest domain ($720 \times 270\,km^2$) covers approximately the extent of southern Norway and the innermost domain ($42.5 \times 42.5\,km^2$) covers a limited area centred around the city of Bergen. There are 61 vertical terrain following sigma levels with an increased density towards the ground and the lowest level is at approximately 36 m above the ground level. The prognostic variables for temperature, humidity and wind are vertically staggered implying that they are calculated at each model half-level with the lowermost at an altitude of approximately 19.5 m above the ground. The two simulations cover respectively the 24-hour periods of 10–11 January 2009 and 25–26 December 2011 of which the first 6 hours are considered as spin-up. The RRTM scheme (Mlawer et al., 1997) is used for long-wave radiation, the Dudhia scheme (Dudhia, 1989) for short-wave radiation, and the Unified NCEP/NCAR/AFWA Noah land-surface model (Chen and Dudhia, 2001) with soil temperature and moisture in four layers for surface physics. Furthermore, the Mellor Yamada Janjic scheme (1990, 1996, 2001) is used for the parameterisation of the boundary layer. The WSM 3-class simple ice scheme (Dudhia, 1989; Hong et al., 2004) is chosen for the parameterisation of microphysics

Table 2. Table used in this study to convert GlobCorine land-use categories to USGS land-use categories

	GlobCorine categories	USGS categories
1	Urban and associated areas	Urban and built-up land
2	Rain-fed cropland	Dryland and cropland pasture
3	Irrigated cropland	Irrigated cropland and pasture
3	Complex cropland	Irrigated cropland and pasture
4	Not converted	Mixed dryland/irrigated cropland and pasture
5	Mosaic cropland/natural vegetation	Cropland/grassland mosaic
6	Mosaic of natural vegetation	Cropland/woodland mosaic
7	Grassland	Grassland
8	Heathland and sclerophyllus vegetation	Shrubland
9	Not converted	Mixed shrubland/grassland
10	Not converted	Savanna
11	Not converted	Deciduous needleleaf forest
12	Not converted	Deciduous broadleaf forest
13	Not converted	Evergreen broadleaf forest
14	Not converted	Evergreen needleleaf forest
15	Forest	Mixed forest
16	Water bodies	Water bodies
17	Vegetated low lying areas on regularly flooded soil	Herbaceous wetland
18	Not converted	Wooded wetland
19	Sparsely vegetated area	Barren or sparsely vegetated
20	Not converted	Herbaceous tundra
21	Not converted	Wooded tundra
22	Not converted	Mixed tundra
23	Not converted	Bare ground tundra
24	Permanent snow and ice	Snow or ice

with cloud water/ice, and rain/snow as prognostic variables. Operational analysis from the European Centre for Medium-Range Weather Forecasts (ECMWF) with a horizontal resolution of 0.125° and 91 vertical model levels is used to initialise and force the model at its boundaries every 6 hours. Additional simulations were performed using ECMWF pressure-level data with a horizontal resolution of 0.5° and 26 vertical levels. These simulations revealed only a very small sensitivity to the initial and lateral boundary conditions.

2.4. The simulation results

2.4.1. Sensitivity to model topography and land-use data
We have carried out a number of sensitivity experiments in this study. The first set of experiments concerns the land use and topography data sets. These are the data sets describing the physiographical model surface in terms of land coverage of, for example, sea, forest, agricultural landscape and urban areas, and topography height. The land use determines to a large extent the local surface energy and momentum budgets. Of probably the greatest importance to this study, which is focused on strong wind speeds, are accurate descriptions of the surface roughness length for momentum (z_0). The roughness is not only highly variable in space, but also in time as a result of changes in urbanisation and vegetation and these are among the main points of interest in the comparison of the different land-use data sets. In WRF, z_0 is along with the albedo, the emissivity and other parameters prescribed for each land-use type using a lookup table.

The most frequently used land-use data set in WRF originates from the United States Geological Survey (USGS) and has a horizontal resolution of approximately 1 km (30 arc seconds). For high-resolution simulations, the resolution and accuracy of this data set is previously found to be insufficient (e.g. Cheng and Byun, 2008; Arnold et al., 2012). To further investigate the validity of this finding to this study, a new data set from GlobCorine is used in an additional set of sensitivity experiments. This data set is based on data from 2009 and is thus of newer date than the USGS data set (1992–1993). GlobCorine has a horizontal resolution of approximately 300 m and it has fewer land-use categories than the USGS set (13 vs. 24). In this study, we use the same lookup table for albedo, roughness, etc. for the GlobCorine data as for the USGS data set. Each land-use category in the GlobCorine data set has been manually adopted to its closest approximate in the USGS data set, meaning that, for example, the GlobCorine 'forest' has been set to 'mixed forest' and so on. A complete list of these conversions is given in Table 2.

The roughness lengths for both the land-use data sets as well as the true roughness length at each of the AWSs are indicated in Fig. 4. The true roughness length is estimated by using the values from the WRF lookup table that correspond to the realistic land-use category at the location of each AWS.

Figure 5 shows the land use over a zoom-in of the finest model domain (500-m horizontal resolution) for the USGS and GlobCorine data sets. It can be seen that, even though GlobCorine has fewer categories, it displays significantly more fine-scale spatial details in the land use field. Also, the

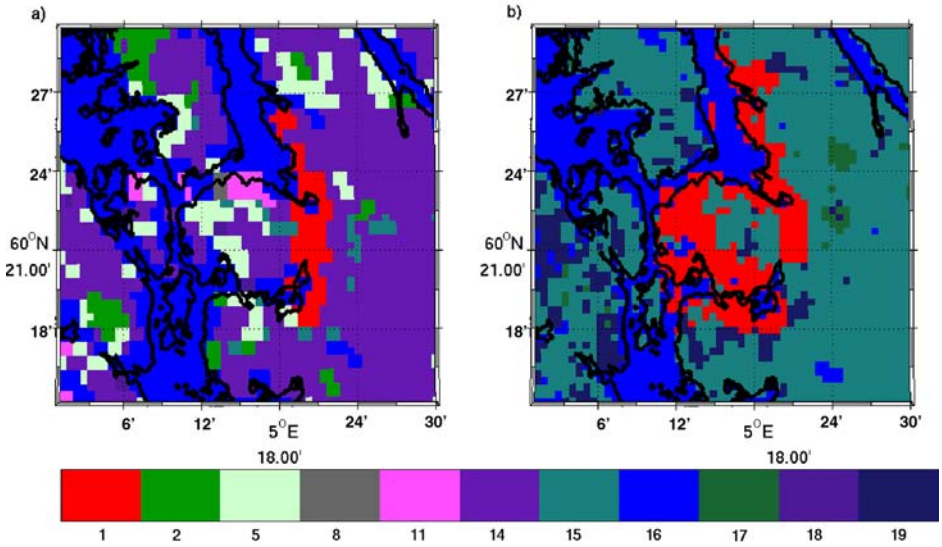

Fig. 5. A zoom-in of the land-use of domain 3 (500-m horizontal resolution) using the data sets of (a) USGS and (b) GlobCorine. See Table 2 for a list over land-use categories and respective numbers indicated on the colour bar. The coastline from Global Self-consistent, Hierarchical, High-resolution Shoreline Database (GSHHS) is indicated with a solid, black line.

Table 3. Weather Research and Forecasting model sensitivity experiments with different land-use and topography data sets

Name	Land use	Topography
USUS	USGS	USGS
USAS	USGS	Aster
GLUS	GlobCorine	USGS
GLAS	GlobCorine	Aster

See text for further explanations.

GlobCorine coastline matches the high-resolution coastline from the Global Self-consistent, Hierarchical, High-resolution Shoreline Database (GSHHS), significantly better than does the USGS coastline.

In addition to the USGS topography data set, we employ a topography data set from the Advanced Spaceborne Thermal Emission and Reflection Radiometer (ASTER). The data set is made in a joint effort between the Ministry of Economy, Trade, and Industry (METI) of Japan and the United States National Aeronautics and Space Administration (NASA). The horizontal resolution is 1 arc second (30 m) as opposed to the 30 arc seconds of the USGS topography data set. We have made a couple of adjustments to the USGS topography and GlobCorine land use data sets. The USGS topography data set features in its standard WRF setup an apparent westwards shift of approximately 500 m when compared to reality (AWS station heights) and the ASTER data set. We therefore corrected it accordingly in the preprocessing of the model data input. Also, a smaller area (approximately 1×1 km) surrounding Nordnes does not have an urban land-use category in the GlobCorine data set. As this area is a part of the centre of Bergen, which is of central interest to this study, the error was corrected accordingly.

The main results from the land-use and topography sensitivity experiments are presented in Fig. 6. The figure shows the average root mean-squared error (RMSE) and mean error (bias) between the available AWS wind speed observations and the corresponding model point estimations.

The error statistics reveal only a marginal sensitivity to the applied model land use and topography data sets. In Case 1, using the GLAS setup gives both the lowest average RMSE (2.4 m s^{-1}) and the lowest average bias (1.3 m s^{-1}). In Case 2, there is no such consistent improvement for any of the experiments. Relatively large wind speed biases are found at Mount Ulriken, with the largest ones being around 6 m s^{-1} in the USUS setup for Case 2. Using the high-resolution terrain data set from ASTER has a clear advantage over using the USGS data

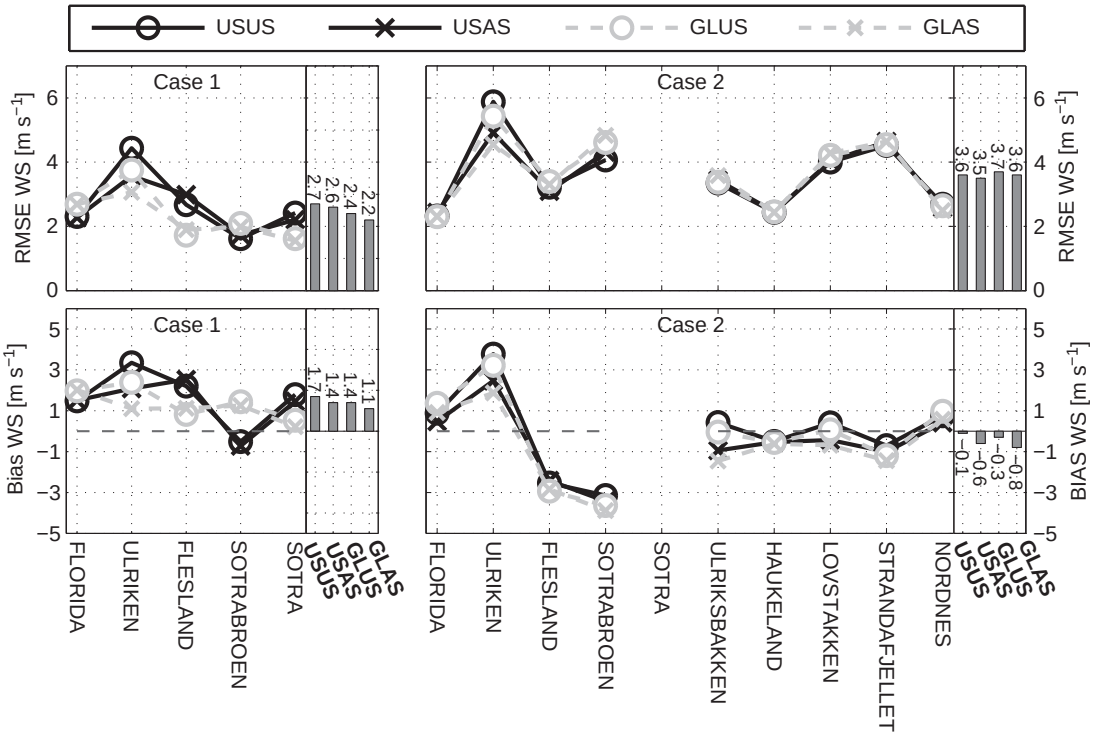

Fig. 6. Root mean-squared error (RMSE) and mean error (bias) for wind speed (observed minus simulated) using four different combinations of model land-use and topography data sets. Table 3 lists and explains the different experiments. Case 1 is 10 January 2009 and Case 2 is 25 December 2011.

set for Ulriken. At this location, there is a reduction in the wind speed RMSE and bias of around 1 m s^{-1} in both cases. In the further analysis of the model results, the GLAS setup is used, which combines the two highest resolution data sets (GlobCorine and ASTER).

2.5. *The Bergen shelter*

The simulated larger scale flow (Fig. 7) compares reasonably well with surface stations situated along the south Norwegian coast. The synoptic flow pattern in south-western Norway did not change much during the course of the day in Case 1. However, the flow during Case 2 started out as south-westerly and ended as westerly. The simulation results show that both cases are associated with strong wind with more than 30 m s^{-1} off the north-western corner (west cape) and over the central mountain range of southern Norway (Langfjella). These flow patterns are typical for south-westerly storms in the region (Barstad and Grønås, 2005).

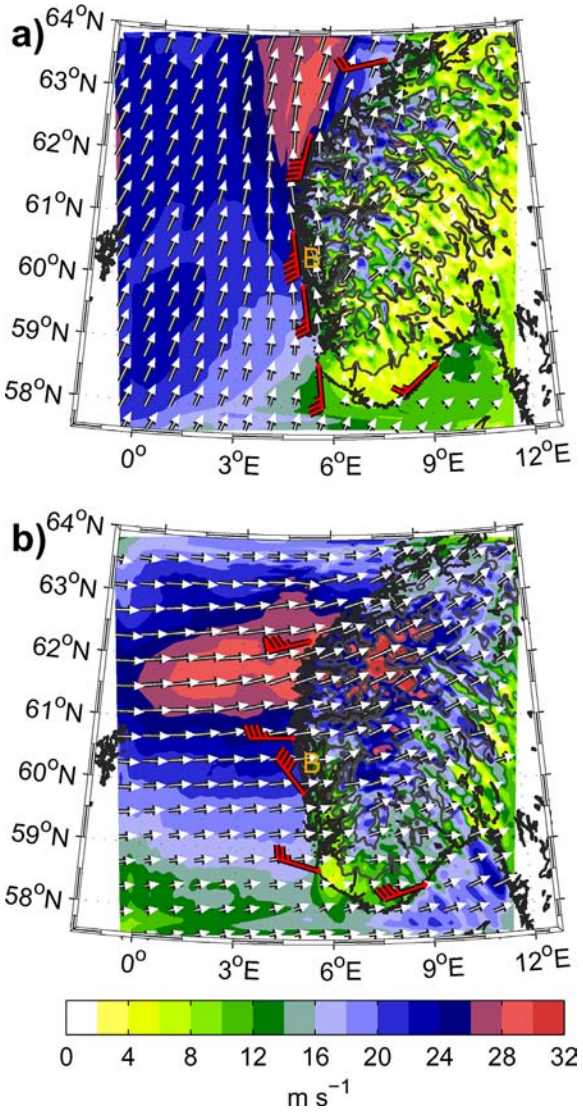

Fig. 7. Simulated near-surface (19.5 m.a.g.l.) horizontal wind speed at (a) 1200 UTC on 11 January 2009 and at (b) 2100 UTC on 25 December 2011. The results are from the outermost domain (4.5-km horizontal resolution). Observations from selected AWSs along the coast are indicated with red wind barbs. Each barb is 2.5 m s^{-1}. The location of Bergen is indicated with a 'B'.

In the Bergen area, the model matches in general the near-surface observed wind speed and wind direction well (Figs. 8 and 9). As commented on in the above error statistics analysis, the largest average deviations are found at Mount Ulriken. Also the simulated wind direction at Ulriken is off by some 20° towards the south in both cases. The model times quite accurately the shift from southerly winds before 1500 UTC to more westerly winds towards the evening in Case 2. An exception is Florida, where this shift happens 2–3 hours earlier in the model than in the observations. The wind speed at Florida is, however, less than 5 m s^{-1} at this time. As described in Section 2.1, this shift in wind direction occurred because the low pressure system that set up the corresponding larger scale flow moved eastwards (Fig. 1).

A main goal of this article is to investigate how the mountains surrounding the centre of Bergen impact the local flow field in the south-westerly storms. We have done this through three different sensitivity experiments, in which the following modifications to the model topography have been applied (see Fig. 2): (1) the Løvstakken massif is removed (NOL), (2) the Fløyen massif is removed (NOF) and (3) both of them are removed (NOFL). The results from these experiments are presented in the following sections.

From Fig. 10, showing the near-surface wind speed at 0000 UTC on 11 January 2009, in the CTRL run and the difference between this and the three topography sensitivity experiments, several deductions can be drawn. First, the simulated local flow field evidently features a considerable spatial variability (Fig. 10a) ranging from 2 to 20 m s^{-1}, thus supporting the impression given from the above analysis of the AWS observations. The highest wind speeds are found along the coast and at the mountain tops. The lowest wind speeds are found immediately up and downstream of the local mountains and hills. The centre of Bergen appears to be one of the calmer areas. Removing the mountain massif of Løvstakken (Fig. 10b) gives a wind speed increase in most parts of the centre of Bergen of 2–6 m s^{-1}. The highest increase is found closest to the massif itself. Removing Fløyen (Fig. 10c) causes a wind speed increase of up to 6 m s^{-1} in an area immediately upstream of the massif. When removing both massifs (Fig. 10d),

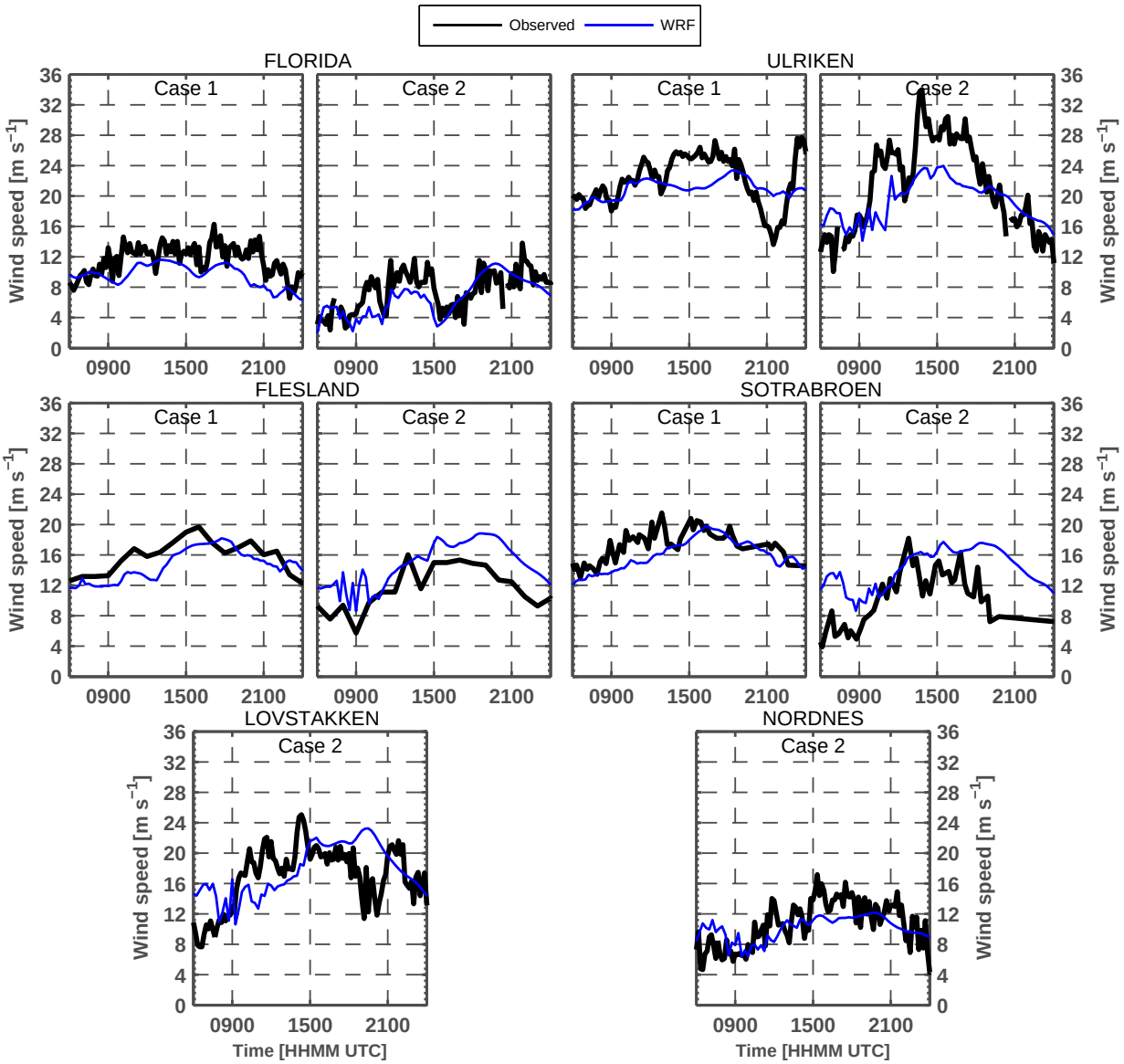

Fig. 8. Observed and simulated wind speed at selected AWSs on 10 January 2009 (Case 1) and 25 December 2011 (Case 2). The simulation results are from the innermost domain (500-m horizontal resolution).

the effect on the wind field in the Bergen valley is the largest and wind speed increases of up to 8 m s^{-1} are seen over larger parts of the city centre. The wind field in the northernmost part of the city centre (around the AWS at Nordnes) is least affected by the model topography modifications.

The above findings allow for the definition of four areas with characteristic flow patterns during the large-scale south-westerly flow, as indicated in Fig. 11: The 'Wake area' is the area immediately downstream of Løvstakken, which is mainly affected by this massif. The 'Less calm area' experiences the smallest effect of the surrounding mountains. The 'Block area' is mainly affected by 'Fløyen' and the 'Florida area', which is the area representative for the main AWSs in the centre of Bergen, is affected by both the presence of Løvstakken and Fløyen. The temporal development of changes in wind speed within each of the areas, as caused by the topography modifications, is shown in Fig. 12. The situation is fairly stationary in most of Case 1, with a slight tendency towards an increased shelter effect and a more westerly synoptic flow towards the end of the day. In Case 2, there is a complete change in wind speed within the four areas at around 1600 UTC as the synoptic wind turns from south-west to west. The area categorisation made above for the south-westerly wind no longer holds for the westerlies.

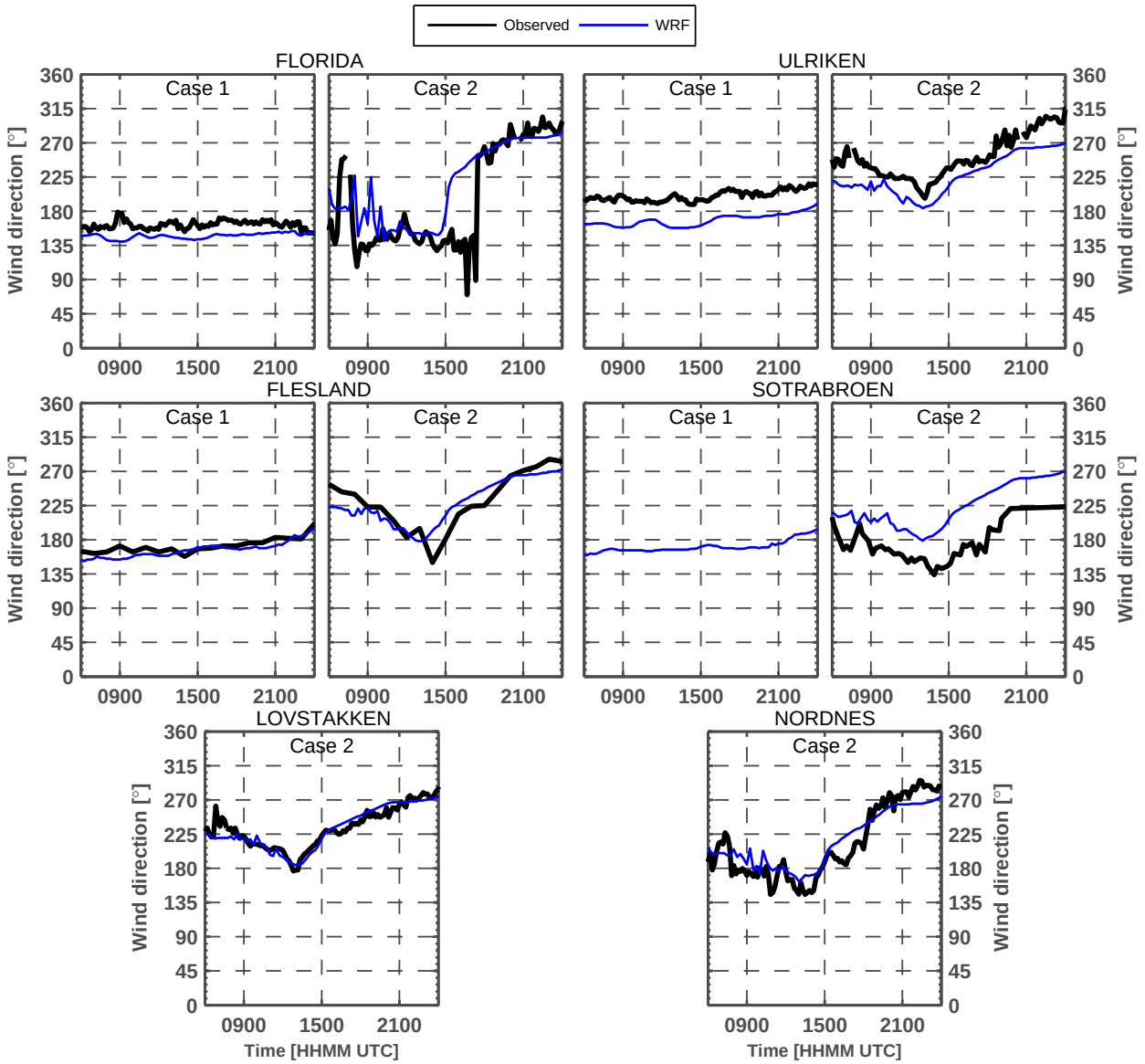

Fig. 9. Observed and simulated wind direction at selected AWSs on 10 January 2009 (Case 1) and 25 December 2011 (Case 2). The simulation results are from the innermost domain (500-m horizontal resolution).

The location of the area affected by Løvstakken shifts further to the south (Fig. 13). However, Fløyen affects an area further to the north and the effect of removing both mountain massifs resembles a superposition of the two former effects. Otherwise, for the south-westerly flow at the beginning of Case 2, the spatial flow patterns seen for the topography modifications resemble closely to that of Case 1 (not shown).

2.6. *The vertical flow structure*

As in the above-described horizontal near-surface wind field, the wind speed reduction in the vertical is largest immediately down and upstream of Løvstakken and Fløyen, respectively (Fig. 14). The vertical extent of the effect from removing Løvstakken is relatively low when compared to the effect from removing Fløyen, which extends to levels roughly twice that of the nearby mountain tops. Upstream of Løvstakken, there is a sign of a small blocking effect ($\geq 2\,\mathrm{m\ s^{-1}}$), which extends to elevations between 1.5 (NOL) and 2 times (NOFL) the height of this mountain.

The combined effect of removing both mountain massifs (NOFL, Fig. 14d) is close to the effect of the blocking alone and it is strongest at around 50 m.a.g.l., where it reduces the wind speed by up to $8\,\mathrm{m\ s^{-1}}$. Above all mountain

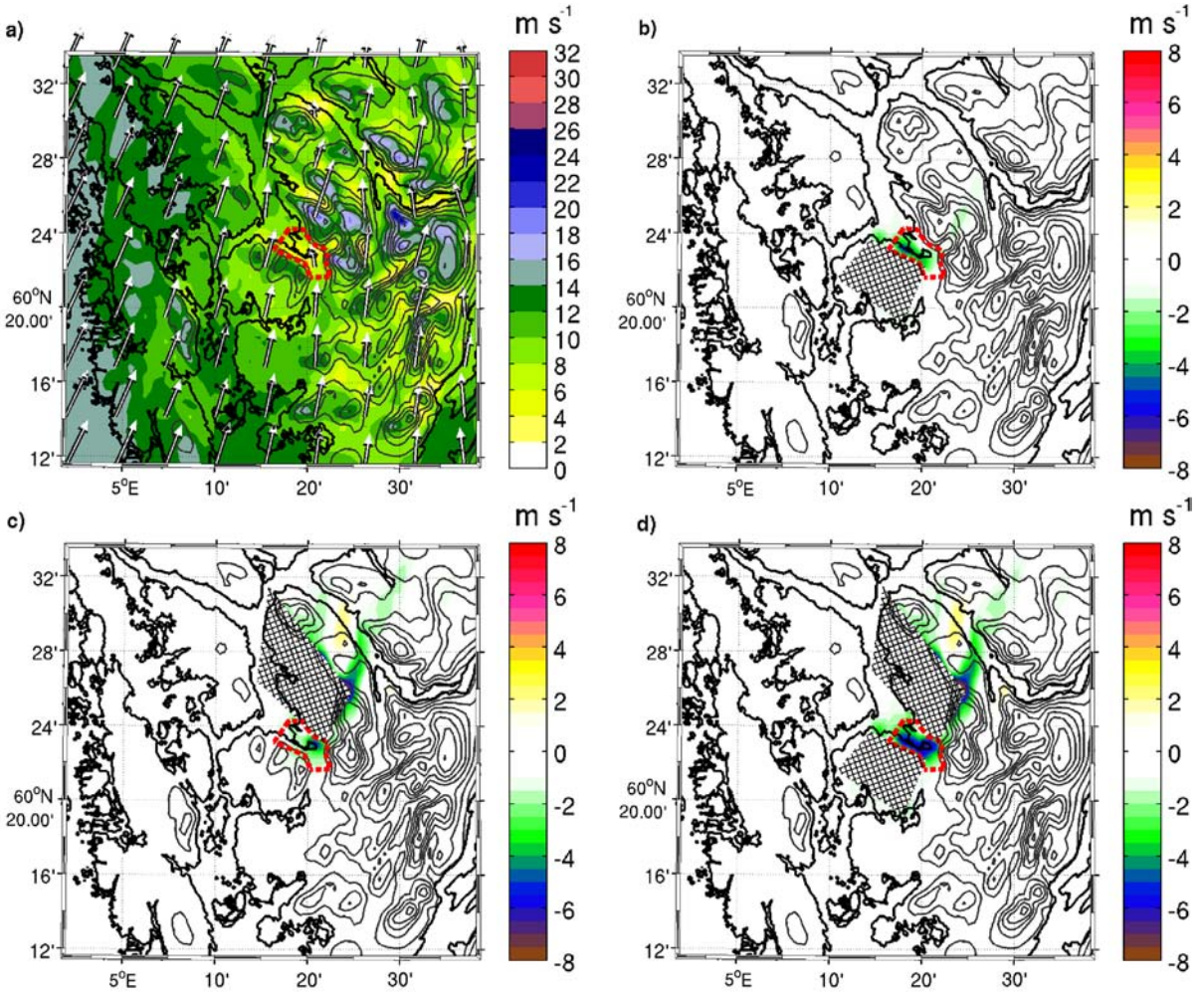

Fig. 10. (a) Near-surface wind speed at 0000 UTC on 11 January in the CTRL simulation, (b) wind speed in CTRL minus NOL, (c) wind speed in CTRL minus NOF and (d) wind speed in CTRL minus NOFL. The dashed, red line indicates the approximate extent of the centre of Bergen.

crests, there are signs of speedup when comparing the runs with and without the true model topography.

2.7. Impact of the local topography on the precipitation field

It is evident that the local topography surrounding Bergen should have an impact on the precipitation in the area. Although precipitation is not the main focus of this article, a short analysis of this parameter is presented. Figure 15 shows the simulated precipitation accumulated between 0600 and 2400 UTC on 10 January 2009. The largest precipitation amounts are found downstream of the local mountain- and hilltops. In most of the centre of Bergen, the simulated 18-hour accumulated precipitation is between 15 and 20 mm, which compares quite well with the observed amount at Florida of 18 mm. In the flat area immediately upstream of Løvstakken, the model predicts only roughly half of this amount. Removing Løvstakken from the model topography (Fig. 15b) brings the amount of precipitation down by 10–12 mm in most parts of the city centre. However, removing Fløyen has barely any impact at all (Fig. 15c). The results for Case 2 are similar to those of Case 1, with no effect on the precipitation in Bergen from removing Fløyen and a slightly smaller effect than in Case 1 from removing Løvstakken (not shown).

3. Discussion

In a set of numerical sensitivity experiments, the atmospheric flow during two south-westerly windstorms that hit south-western Norway on 10 January 2009 and 25 November 2011 has been reproduced. The results show that the sheltering of the north-eastern part of the city

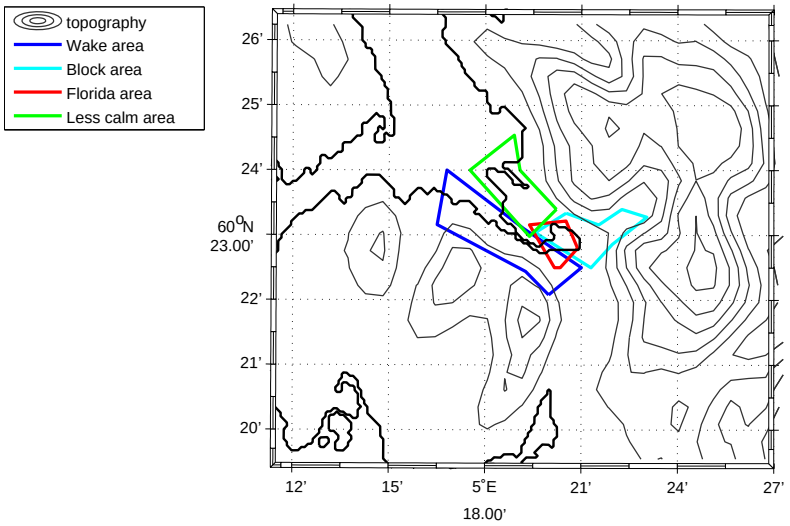

Fig. 11. Areas of characteristic location and flow patterns. The terrain height is given with contours every 100 m.

centre of Bergen is caused by a decelerating effect upstream of the Fløyen massif, while the sheltering in the south-western part of Bergen is largely a wake effect of the Løvstakken massif. These findings seem reasonable as these areas lie close to the foothills of the mountains with the largest impact on the wind. A more interesting result is that the total sheltering effect of both mountains is close to the sum of the blocking effect of Fløyen and the wake effect of

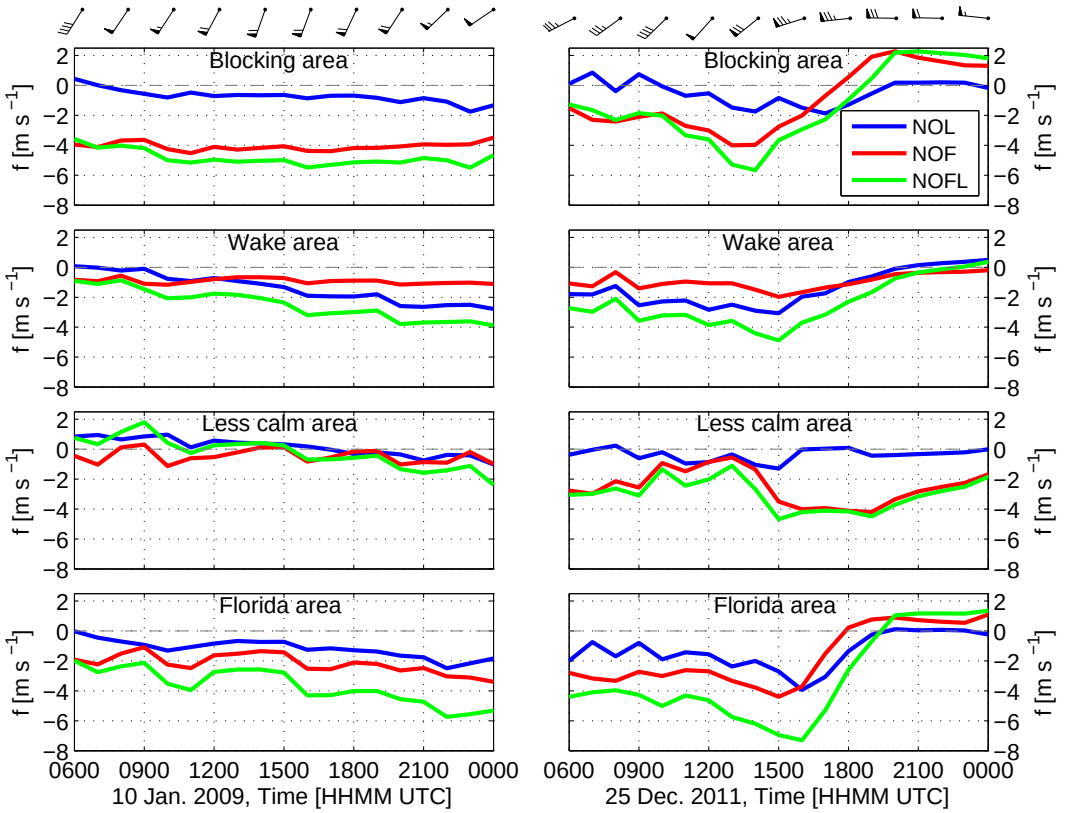

Fig. 12. Difference in simulated near-surface wind speed between the CTRL and the sensitivity simulations with topography modifications averaged within the areas indicated in Fig. 11. The wind barbs at the top of the panels denote the simulated wind speed and direction at 900 hPa averaged within a box centred at 4.3°E and 61°N. Each half barb is 2.5 m s^{-1}.

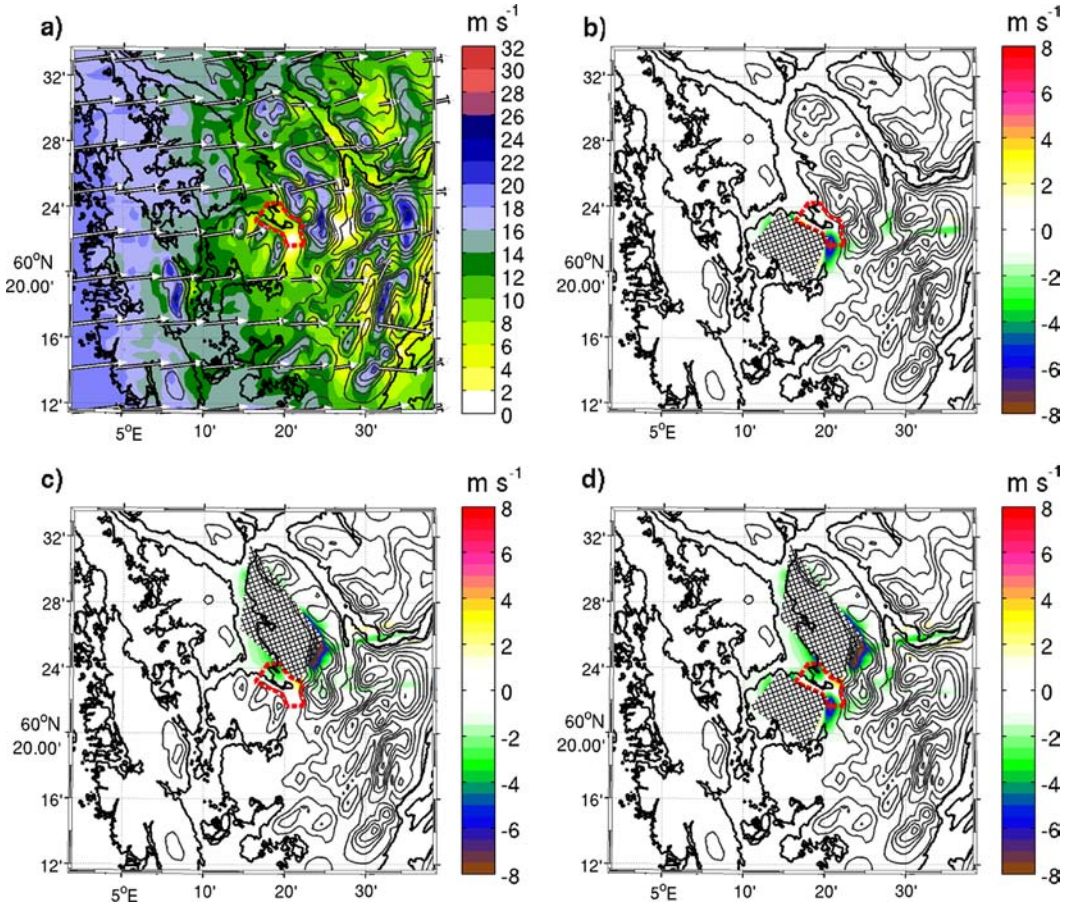

Fig. 13. (a) Near-surface wind speed at 2100 UTC on 25 December 2011 in the CTRL simulation, (b) wind speed in CTRL minus NOL, (c) wind speed in CTRL minus NOF and (d) wind speed in CTRL minus NOFL. The dashed, red line indicates the approximate extent of the centre of Bergen.

Løvstakken. This is roughly valid in all central parts of the city as well as aloft, above the Bergen valley. No existing theory supports this result. There are indeed several studies that reveal that stratified flow in the vicinity of two mountains can be very sensitive to both horizontal and vertical scales of the topography. Through the modification of gravity waves, a mountain downstream of a valley can thus both contribute to acceleration and deceleration of the flow inside the valley. Such effects have been studied by, for example, Hunt and Richards (1984), Grubišić and Stiperski (2009), and Stiperski and Grubišić (2011) for idealised flows and Ágústsson and Ólafsson (2007) for real flows. Seen from an energetic point of view, a reduction of the speed or the kinetic energy by the wake of the first mountain moves the flow deeper into a regime of orographic blocking as it meets the second mountain and the non-dimensional mountain height is increased. A wake may also be enhanced or sustained by a downstream mountain, blocking the low-level flow.

The simulated near-surface wind speed compares relatively well with the observations from a local AWS network. A sensitivity analysis using two different model topography data sets (USGS and ASTER) and two different land-use data sets (USGS and GlobCorine) shows only a marginal sensitivity in the wind speed error statistics to the choice of these data sets. Previous studies have found larger differences when comparing lower and higher resolution data sets (e.g. Cheng and Byun, 2008; Arnold et al., 2012). One consistent improvement, however, is seen in the wind speed at Ulriken when applying the ASTER topography data set instead of the USGS topography data set. This improvement is most likely caused by a more accurate description of the topography in the ASTER data set. In reality, the Ulriken AWS is situated at 605 m.a.s.l., whereas in the simulations using the USGS data set it is at 459 m.a.s.l. and in those using the ASTER data set it is at 470 m.a.s.l. In a study of extreme winds in the Bergen region, Harstveit (2006) asserted that Ulriken

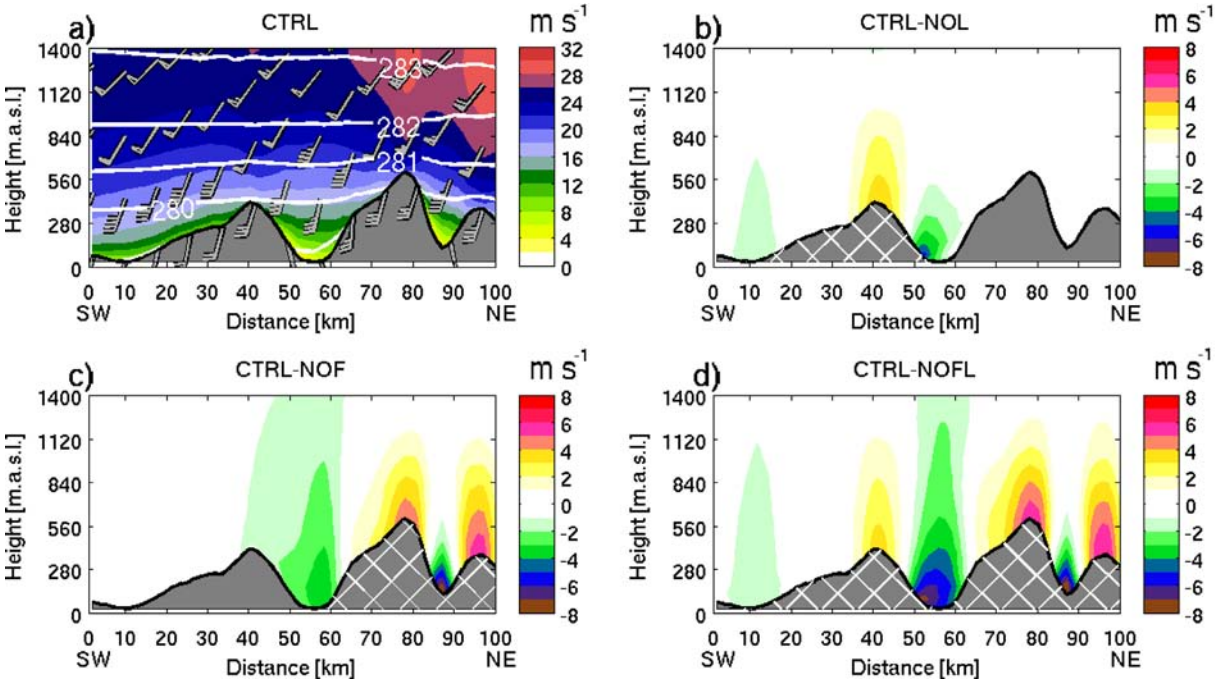

Fig. 14. (a) Cross section of horizontal wind speed at 0000 UTC on 11 January in the CTRL simulation, (b) wind speed in CTRL minus NOL, (c) wind speed in CTRL minus NOF and (d) wind speed in CTRL minus NOFL. The geographical location of the cross section is indicated in Fig. 2.

experiences a local speed up of winds from the sector south to west. He attributed this speed-up to small-scale features in the local terrain. It is evident that a simulation, even at a high horizontal resolution of 500 m, will not accurately capture all such local features. Larger improvements from using higher resolution topography model data sets can probably be expected when going to even higher horizontal grid resolutions. Then, however, one approaches scales at which the normal ABL model schemes are no longer suited and Large-Eddy Simulation (LES) schemes should rather be applied. Such simulations are beyond the scope of this study.

Although the studied windstorms are quite typical in terms of wind pattern (see climatology by Jonassen et al., 2012), there do exist cases where strong and gusty winds in south-westerly flow reach down to parts of the centre of Bergen (e.g. Harstveit, 2006). Such cases are, however, not common and they are presumably related to rare details in the vertical profile of the flow and are left for future studies.

A significant downstream shift of the precipitation maximum around the mountain massif of Løvstakken, largely affecting the city centre of Bergen, is found in the simulation of the south-westerly windstorm of 10 January 2009. This 'spillover effect' is typical for strong wind events as described by, for example, Sinclair et al. (1997) and during the Reykjanes experiment described in Rögnvaldsson et al. (2007). The removal of Løvstakken from the model topography confirms that this mountain is the source of the described precipitation pattern. Removing the Fløyen mountain massif, which is downstream of the city centre, has hardly any effect on the precipitation in the city. When compared to many of the surrounding mountains and especially the South Norwegian mountain range as a whole, Løvstakken is a relatively narrow mountain. Narrow mountains are known to be associated with a stronger spillover effect than wider ones (e.g. Colle and Zeng, 2004) as they allow for a relatively low residence time for hydrometeor growth. Wider mountains give hydrometeors longer time for growth, interaction and fallout over the windward slope (Jiang, 2003). Both our cases are dominated by a fairly neutrally stratified atmosphere. Following the results by Sinclair et al. (1997) on spillover and atmospheric stability, a stronger atmospheric stability would presumably lead to a decreased spillover effect over Løvstakken while a decreased stability would have the opposite effect. A higher mountain would also lead to more of the flow going around rather than over the mountain and thereby reduce the spillover. A higher hydrometeor fall velocity would also most likely reduce the spillover effect with more precipitation falling down on the upstream rather than on the downstream side of the mountain crest.

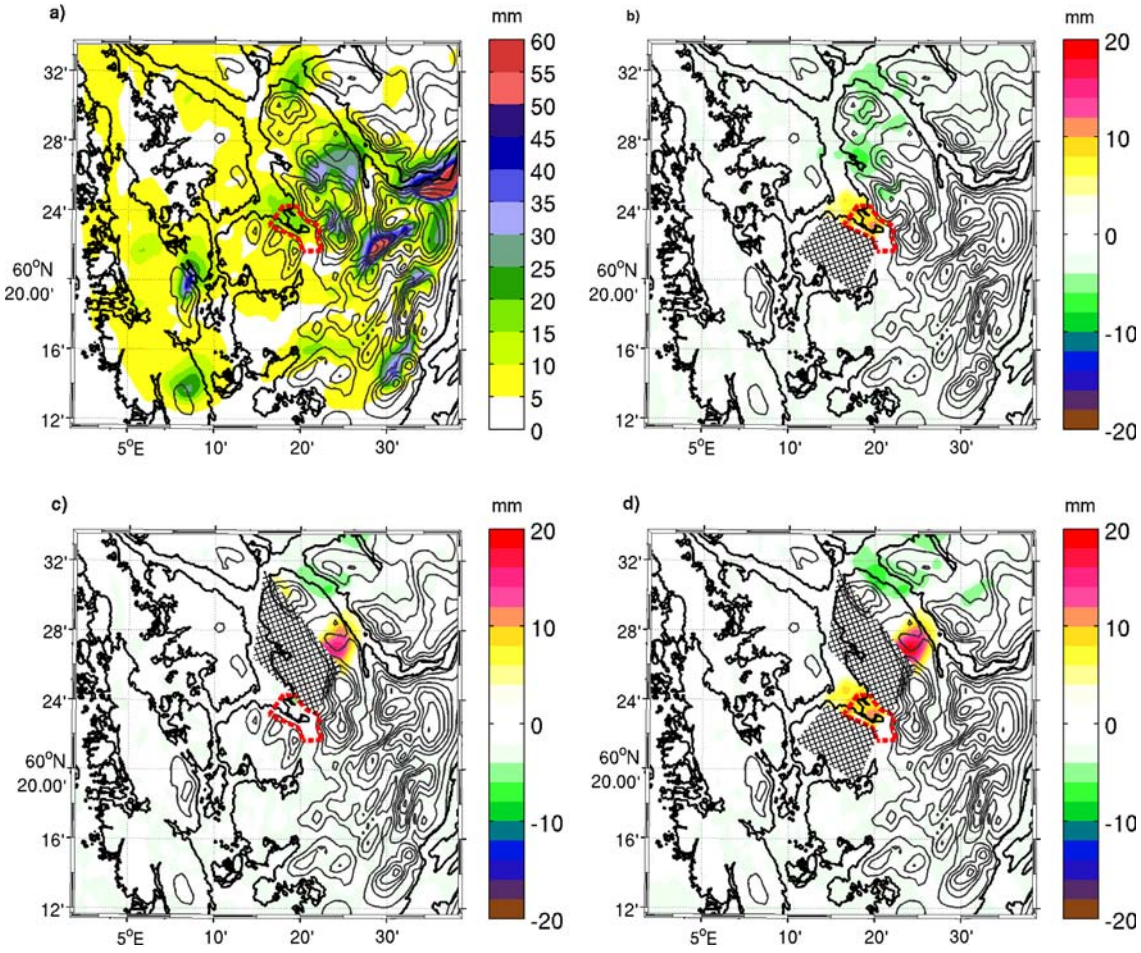

Fig. 15. (a) 18-hour accumulated precipitation at 0000 UTC on 11 January 2009, in the CTRL simulation, (b) precipitation in CTRL minus NOL, (c) precipitation in CTRL minus NOF and (d) precipitation in CTRL minus NOFL.

Previous simulations of orographic precipitation with a clear spillover, as, for example, Rögnvaldsson et al. (2007), have revealed a limited sensitivity of the precipitation pattern to the choice of microphysics parameterisation scheme. The topographic and atmospheric conditions in Rögnvaldsson et al. (2007) were quite similar to those in this study, but in order to establish a conclusive and quantitative result on the impact of individual mountains of the precipitation climatology many more simulations would be needed. More simulations could also allow for a more detailed quantification of the relative role of the smaller scale topography with respect to that on larger scale on the precipitation in the area. In our cases with strong winds, the effect from the local mountains on the precipitation seems to dominate over the larger scale topography through a spillover effect. For other cases, for example, with lower wind speeds which are far more common in the area than windstorms, the larger scale topography may play a greater role.

4. Summary and conclusions

In this study, our main goal has been to investigate why the centre of Bergen is sheltered during south-westerly windstorms. A series of numerical sensitivity experiments, in which we have removed stepwise larger parts of the topography surrounding the city centre from the model topography during two south-westerly windstorms, give some answers. The sheltering of Bergen appears to be caused by a combination of a downstream wake of the Løvstakken mountain massif and an upstream blocking from the Fløyen massif. The combined effect is close to the sum of each of them.

Regarding the initially posed question whether the AWS at Florida is representative of the Bergen centre as a whole, this is only partly true. The effect from each of the mountains is strongest closest to their foothills. Hence, downstream of Løvstakken a wake dominates and upstream of Fløyen, there is a zone of blocking.

At Florida, the blocking effect from Fløyen is most prominent.

Through spillover, the Løvstakken massif acts to increase the precipitation in the centre of Bergen during both of the investigated windstorms. The Fløyen massif turns out to have a minimum impact on the precipitation upstream of it. The strength of the spillover effect is known to increase with increasing wind speeds. Thus, the effect is likely less pronounced on the average than in the present strong wind cases.

A series of numerical sensitivity experiments using high-resolution land-use and topography data sets have been carried out. The wind speed error statistics reveal only a marginal sensitivity to the choice of these data sets. This result may, however, be sensitive to the horizontal grid resolution.

5. Acknowledgments

This study is partly the result of a long-lasting collaboration between Aanderaa Data Instruments and GFI on weather observations at Mount Ulriken. The authors also owe their gratitude to Avinor and met.no for giving access to data from Sotra.

References

Ágústsson, H. and Ólafsson, H. 2007. Simulating a severe windstorm in complex terrain. *Meteorol. Z.* **16**(1), 111–122.

Andersen, F. 1975. Surface winds in southern Norway in relation to prevailing H. Johansen weather types. *Meteor. Ann.* **6**(14), 377–399.

Arnold, D., Schicker, I. and Seibert, P. 2012. Towards high-resolution environmental modelling in the alpine region. *NATO Sci. Peace Security Series C: Environ. Security*. **14**, 269–273.

Barstad, I. and Grønås, S. 2005. Southwesterly flows over southern Norway-Mesoscale sensitivity to large-scale wind direction and speed. *Tellus A*. **57**, 136–152.

Barstad, I. and Grønås, S. 2006. Dynamical structures for southwesterly airflow over southern Norway: the role of dissipation. *Tellus A*. **58**, 2–18.

Berge, E. and Hassel, F. 1984. *An Investigation of Temperature Inversions and Local Drainage Flow in Bergen, Norway* (in Norwegian). Meteorological Report Series, University of Bergen, Bergen, Norway.

Bjerknes, J. and Solberg, H. 1921. Meteorological conditions for the formation of rain. *Geofys. Publ.* **2**(3), 3–60.

Bjerknes, J. and Solberg, H. 1922. Life cycles of cyclones and polar front theory of the atmospheric circulation. *Geofys. Publ.* **3**(1), 1–18.

Chen, F. and Dudhia, J. 2001. Coupling an advanced land surface-hydrology model with the Penn State-NCAR MM5 modeling system. Part 1. Model implementation and sensitivity. *Mon. Wea. Rev.* **129**, 569–585.

Cheng, F.-Y. and Byun, D. W. 2008. Application of high resolution landuse and land cover data for atmospheric modeling in the Houston–Galveston metropolitan area, Part I: meteorological simulation results. *Atmos. Environ.* **42**, 7795–7811.

Colle, B. A. and Zeng, Y. 2004. Bulk microphysical sensitivities within the MM5 for orographic precipitation. Part II: impact of barrier width and freezing level. *Mon. Wea. Rev.* **132**, 2802–2815.

Dudhia, J. 1989. Numerical study of convection observed during the winter monsoon experiment using a mesoscale two-dimensional model. *J. Atmos. Sci.* **46**, 3077–3107.

Grubišić, V. and Stiperski, I. 2009. Lee-wave resonances over double bell-shaped obstacles. *J. Atmos. Sci.* **66**, 1205–1228.

Harstveit, K. 2006. Mapping of extreme wind conditions in Bergen kommune (in Norwegian). *met.no report* 3, Norwegian Meteorological Institute, 55 pp. Online at: http://met.no/filestore/report03_06.pdf

Hong, S., Dudhia, J. and Chen, S. 2004. A revised approach to ice microphysical processes for the bulk parameterization of clouds and precipitation. *Mon. Weather Rev.* **132**, 103–120.

Hunt, J. C. R. and Richards, K. J. 1984. Stratified airflow over one or two hills. *Bound.-Layer Meteorol.* **30**, 223–229.

Janjic, Z. 1990. The step-mountain coordinate: physical package. *Mon. Weather Rev.* **118**, 1429–1443.

Janjic, Z. 1996. The surface layer in the NCEP eta model. In: *11th Conference on Numerical Weather Prediction*, Norfolk, VA, 19–23 August; American Meteorological Society, Boston, MA, 354–355.

Janjic, Z. 2001. *Nonsingular Implementation of the Mellor-Yamada Level 2.5 Scheme in the NCEP Meso Models*. Office Note 437, National Centers for Environmental Prediction, 61 pp.

Jiang, Q. 2003. Moist dynamics and orographic precipitation. *Tellus A*. **55**, 301–316.

Jonassen, M. O., Ólafsson, H., Reuder, J. and Olseth, J. A. 2012. Multi-scale variability of winds in the complex topography of southwestern Norway. *Tellus A*. **64**, 1–17.

Lin, Y.-L. and Wang, T.-A. 1996. Flow regimes and transient dynamics of two-dimensional flow over an isolated mountain ridge. *J. Atmos. Sci.* **53**, 139–158.

Mlawer, E. J., Taubman, S. J., Brown, P. D., Iacono, M. J. and Clough, S. A. 1997. Radiative transfer for inhomogeneous atmospheres: RRTM, a validated correlated-k model for the longwave. *J. Geophys. Res.* **102**, 16663–16682.

Ólafsson, H. and Bougeault, P. 1996. Nonlinear flow past an elliptic mountain ridge. *J. Atmos. Sci.* **53**, 2465–2489.

Peng, M. S., Li, S.-W., Chang, S. W. and Williams, R. T. 1995. Flow over mountains: coriolis force, transient troughs and three dimensionality. *Q. J. R. Meteorol. Soc.* **121**, 593–613.

Pierrehumbert, R. and Wyman, B. 1985. Upstream effects of mesoscale mountains. *J. Atmos. Sci.* **42**, 977–1003.

Reuder, J., Fagerlid, G. O., Barstad, I. and Sandvik, A. 2007. Stord Orographic Precipitation Experiment (STOPEX): an overview of phase I. *Adv. Geosci.* **10**, 17–23.

Rögnvaldsson, O., Bao, J.-W. and Ólafsson, H. 2007. Sensitivity simulations of orographic precipitation with MM5 and

comparison with observations in Iceland during the Reykjanes Experiment. *Meteorol. Z.* **16**, 87–98.

Sinclair, M. R., Wratt, D. S., Henderson, R. D. and Gray, W. R. 1997. Factors affecting the distribution and spillover of precipitation in the Southern Alps of New Zealand – a case study. *J. Appl. Meteor.* **36**, 428–442.

Skamarock, W. C., Klemp, J. B., Dudhia, J., Gill, D. O., Barker, D. M. and co-authors. 2008. *A Description of the Advanced Research WRF Version 3*. NCAR Tech. Note TN-475+STR, 125 pp.

Smith, R. B. 2006. Progress on the theory of orographic precipitation. *Spec. Pap. Geol. Soc. Am.* **398**, 1–16.

Smith, R. B., Gleason, A. C. and Gluhosky, A. 1997. The wake of St. Vincent. *J. Atmos. Sci.* **54**, 606–623.

Spinnangr, F. 1943. Synoptic studies on precipitation in Southern Norway. II: Front precipitation. *Meteor. Ann.* **1**(17), 433–468.

Steensen, B. M., Ólafsson, H. and Jonassen, M. 2011. An extreme precipitation event in Central Norway. *Tellus A.* **63**, 675–686.

Stiperski, I. and Grubišić, V. 2011. Trapped lee wave interference in the presence of surface friction. *J. Atmos. Sci.* **68**, 918–936.

Teigen, R. 2005. *Numerical Simulation of Orographic Precipitation in West Norway* (in Norwegian). PhD Thesis. Geophysical Institute, University of Bergen. Online at: http://www.ub.uib.no/elpub/2005/h/406004/Hovedoppgave.pdf

Trüb, J. and Davies, H. C. 1995. Flow over a mesoscale ridge: pathways to regime transition. *Tellus A.* **47**, 502–524.

Utaaker, K. 1995. *Energy in the Planning of Area – Local Climate in Bergen* (in Norwegian). Meteorological Report Series, University of Bergen.

Valved, A. S. 2012. *Local Flow Conditions in the Bergen Valley Based on Observations and Numerical Simulations*. PhD Thesis. Geophysical Institute, University of Bergen.